

Reactions of Hydroxyl Radical with Humic Substances: Bleaching, Mineralization, and Production of Bioavailable Carbon Substrates

J. V. GOLDSTONE,^{†,‡} M. J. PULLIN,[‡]
S. BERTILSSON,[‡] AND B. M. VOELKER^{*‡}

Marine Chemistry and Geochemistry, Woods Hole
Oceanographic Institution, and Department of Civil and
Environmental Engineering, Massachusetts Institute of
Technology, Cambridge, Massachusetts 02139

In this study, we examine the role of the hydroxyl (OH[•]) radical as a mechanism for the photodecomposition of chromophoric dissolved organic matter (CDOM) in sunlit surface waters. Using γ -radiolysis of water, OH[•] was generated in solutions of standard humic substances in quantities comparable to those produced on time scales of days in sunlit surface waters. The second-order rate coefficients of OH[•] reaction with Suwannee River fulvic (SRFA; $2.7 \times 10^4 \text{ s}^{-1} (\text{mg of C/L})^{-1}$) and humic acids (SRHA; $1.9 \times 10^4 \text{ s}^{-1} (\text{mg of C/L})^{-1}$) are comparable to those observed for DOM in natural water samples and DOM isolates from other sources but decrease slightly with increasing OH[•] doses. OH[•] reactions with humic substances produced dissolved inorganic carbon (DIC) with a high efficiency of $\sim 0.3 \text{ mol of CO}_2/\text{mol of OH}^{\bullet}$. This efficiency stayed approximately constant from early phases of oxidation until complete mineralization of the DOM. Production rates of low molecular weight (LMW) acids including acetic, formic, malonic, and oxalic acids by reaction of SRFA and SRHA with OH[•] were measured using HPLC. Ratios of production rates of these acids to rates of DIC production for SRHA and for SRFA were similar to those observed upon photolysis of natural water samples. Bioassays indicated that OH[•] reactions with humic substances do not result in measurable formation of bioavailable carbon substrates other than the LMW acids. Bleaching of humic chromophores by OH[•] was relatively slow. Our results indicate that OH[•] reactions with humic substances are not likely to contribute significantly to observed rates of DOM photomineralization and LMW acid production in sunlit waters. They are also not likely to be a significant mechanism of photobleaching except in waters with very high OH[•] photoformation rates.

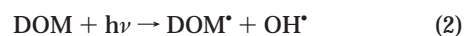
Introduction

Aquatic dissolved organic matter (DOM) is in part composed of light-absorbing polymers that are resistant to microbial assimilation and breakdown. The photodecomposition of this chromophoric DOM (CDOM) in natural waters is of interest for a number of reasons. First, CDOM photolysis

could represent an important source of nutrients and carbon substrates to microorganisms. Biologically available photo-products that have been identified include CO (1); low molecular weight (LMW) organic compounds, including carboxylic acids and carbonyl compounds (2–7); and ammonia (8). Second, CDOM has further ecological significance as the main absorber of UV-A and UV-B radiation in natural waters, shielding aquatic organisms from sunlight's harmful effects (9). Photodecomposition of this material results in the destruction of its light-absorbing properties (photo-bleaching). Finally, photomineralization of CDOM to dissolved inorganic carbon (DIC) may constitute a significant flux in the global carbon cycle (10). In some cases, utilization of photoproduct carbon substrates by bacteria seems to be the more significant pathway to mineralization (11–13), while in other systems abiotic photomineralization of DOM is more significant (10, 14, 15).

Photodecomposition may proceed both via direct photochemical reactions, involving energy and electron transfer after absorption of photons by CDOM, (16–19), or via indirect (sensitized) processes, involving DOM reactions with photochemically generated intermediates such as reactive oxygen species (ROS). The relative importance of these two general classes of mechanisms must be understood in order to be able to utilize laboratory studies of DOM photodecomposition and product formation rates to estimate the rates of these processes in the environment. If direct photochemical processes dominate, only the chromophoric portion of the DOM will be broken down by this mechanism, and the rates of photodecomposition and product formation will be proportional to the amount of light absorbed by the CDOM. If indirect photochemical processes are important, photodecomposition of nonchromophoric material is also possible, and the rate of light absorption by CDOM will only control the rates if CDOM photoreactions are the main source of the intermediates involved. There is no reason to assume that the same general mechanism is responsible for different processes of interest; for instance, photobleaching could proceed mostly via direct mechanisms while photomineralization and photoproduction of LMW organic compounds could proceed mostly via indirect mechanisms.

Of the various reactive intermediates produced in sunlit natural waters, the hydroxyl radical (OH[•]) is the likeliest candidate for having significant effects on DOM decomposition. OH[•] is a powerful oxidant known to react with many organic compounds at nearly diffusion-limited rates. Reaction rate constants of OH[•] with DOM measured in a number of natural water samples and isolates, typically $(1-7) \times 10^4 \text{ s}^{-1} (\text{mg of C/L})^{-1}$ (20–24), imply that DOM is the primary sink of OH[•] in most freshwaters. The rate of DOM oxidation by OH[•] must then be approximately equal to the photoproduction rate of OH[•]. Sources of OH[•] in sunlit waters include nitrate photolysis (22, 25) and DOM photolysis (26) (eqs 1 and 2):



OH[•] production rates are dependent on the concentrations of these sources as well as on the available sunlight. Midday near-surface production rates range from 10^{-13} to $10^{-10} \text{ M s}^{-1}$ in most natural waters, although production rates as high as 10^{-9} M s^{-1} have been observed in samples from the Florida Everglades (27). Steep attenuation of OH[•] production rates

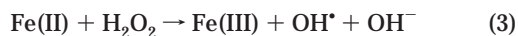
* Corresponding author e-mail: voelker@mit.edu; telephone: (617)253-3726; fax: (617)258-8850.

[†] Woods Hole Oceanographic Institution.

[‡] Department of Civil and Environmental Engineering.

with water depth are expected, as UV irradiation is needed to produce OH[•].

Photo-Fenton reactions, the oxidation of photoproducted Fe(II) by photoproducted HOOH, have also been suggested as a significant source of OH[•] in sunlit natural waters (28, 29) (eq 3):



Ongoing studies in our own laboratory suggest that Fenton's reaction could potentially result in OH[•] photoproduction rates as high as 10⁻⁹ M s⁻¹ in sunlit, organic-rich, iron-rich, mildly acidic waters (30). Increases in OH[•] production rates due to Fenton chemistry may explain observed increases in the rate of photoproduction of DIC and other DOM photoproducts in the presence of Fe (14, 31) as well as positive correlations of photoproduction rates of DIC with Fe content in a number of Swedish lake water samples (12). Alternatively, the Fe effect may be attributable to a direct photochemical process, ligand to metal charge transfer (LMCT) reactions, that entail the oxidation of CDOM with the concurrent reduction of Fe(III) to Fe(II) (29, 31, 32). While Fe effects on LMW acid production were not observed in the Swedish lake study, Mopper and Zhou (27) suggested OH[•] involvement in the photoproduction of LMW carboxyl compounds in seawater.

Although the effects of OH[•] on the decomposition of DOM have not been extensively investigated in natural waters, these reactions have been studied in engineered systems. Both the pulp and paper and the drinking water treatment industries have been interested in the oxidative reactions of OH[•] with organic matter. Hydrogen peroxide (HOOH) has been used as a bleaching reagent in the pulp and paper industry for more than 50 yr (33). Until recently, the perhydroxyl radical anion, HO₂⁻, was believed to be the active species present during alkaline bleaching processes (33, 34). However, a number of studies have shown that OH[•] is an integral part of the bleaching process (34–38).

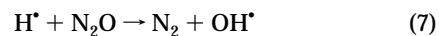
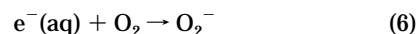
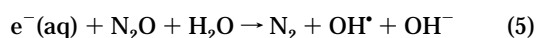
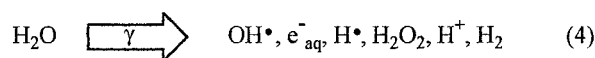
The production of OH[•] is also thought to be one of the important processes occurring during advanced oxidation process (AOP) treatments of paper pulp, wastewater, and drinking water, which replace chlorine-based oxidants with use of ozone, ozone–hydrogen peroxide, UV–ozone, UV–hydrogen peroxide, or photo-Fenton chemistries (39–41). Rapid bleaching and mineralization as well as production of LMW mono- and diacids are observed during ozonation and other AOP and total chlorine-free (TCF) bleaching treatments (35, 42–44). The specific contributions of OH[•] reactions to the observed rates of product formation from DOM decomposition processes has generally not been assessed.

The purpose of this study is to determine whether reactions of DOM with OH[•] play a role in the photomineralization and photobleaching of DOM and the photoproduction of biologically available carbon sources in natural waters. γ -radiolysis of water was used to produce OH[•] nonphotolytically, avoiding the complicating effects of multiple reactions occurring in the DOM matrix and the aqueous solvent during irradiation with light. Rates of bleaching and mineralization of extracted fulvic and humic acid standards (Suwannee River humic and fulvic acids; SRHA and SRFA, respectively) by OH[•] were examined under a range of conditions representative of natural waters. In addition, we have examined the role of OH[•] in the production of LMW organic acids, which are important products of DOM photolysis. Because the production of LMW carboxylic acids is not the only potential effect of OH[•] on DOM bioavailability, we also used dilution cultures with bacterial growth potential as an indirect measure of the impact of hydroxyl radical on DOM substrate quality and bioavailability (45).

Methods

Materials. Suwannee River humic and fulvic acid reference materials (SRHA 1R103H and SRFA 1R101F) were obtained from the International Humic Substances Society. Seawater samples were collected from Delaware Bay using the Teflon flow system of the R/V Cape Henlopen. Samples were 0.45- and 0.2- μm filtered through acid-washed and extensively preirradiated cartridge filters and stored in the dark at 4 °C in fluorinated HDPE carboys. DOC-free seawater was produced by UV irradiating 0.2- μm filtered Sargasso Sea using an air-cooled medium-pressure Hg lamp. Massachusetts Bay water for bacterial growth experiments was sampled at Revere State Beach using an acid-washed Teflon bottle and filtered through precombusted Whatman GF/F filters (3 h at 450 °C, nominal pore-size 0.7 μm). Argon (grade 4.8), oxygen (grade 4.4), CO₂-free air (TOC grade), and N₂O (grade 2) were obtained from BOC Gases. All reagents were purchased from Sigma-Aldrich and used as received unless otherwise specified.

Radiolysis. By γ -radiolysis of N₂O-saturated aqueous solutions, the radiolytic decomposition of water can be exploited to produce a stable, steady flux of OH[•] via the reactions of hydrated electrons (e⁻(aq)) and hydrogen atoms (H[•]) with N₂O (eqs 4–8; 46). In the presence of O₂, the reducing radical H[•] is instead converted into HO₂ (eq 8) (>93% and >98% with 4:1 N₂O/air and N₂O/oxygen mixtures) while the reaction of O₂ with e⁻(aq) is less significant, so that e⁻(aq) is still converted (>99 and >98%, respectively) into OH[•]:



γ -radiolysis was performed using a ⁶⁰Co source (GammaCell-220) emitting 0.13 kGy/h of γ -radiation (1.2 MeV). Dosimetry was performed using the standard Fricke dosimeter (47) and also by measuring hydrogen peroxide production rates using acridinium ester chemiluminescence (48) or the *N,N*-diethyl-*p*-phenylenediamine–peroxidase method (49). Samples were saturated with N₂O or with a 4:1 mixture of N₂O and either CO₂-free air or O₂, transferred under constant gas purge to precombusted amber glass vials with Teflon-lined silicone septa, and irradiated in the GammaCell. The net radiation-chemical yield (*G* value) for OH[•] in the absence of O₂ is 5.9 molecules/100 eV, while in the presence of O₂ it drops to 5.3 molecules/100 eV (46). These values correspond to OH[•] production rates of 1.9 × 10⁻⁸ and 1.7 × 10⁻⁸ M s⁻¹ in N₂O and N₂O/air or oxygen-saturated solutions, respectively. Analyses were performed immediately after irradiation.

Phosphate buffers were used to control the pH of the solutions where indicated. Because the reaction rate constants of phosphate species with OH[•] are all <3 × 10⁶ M⁻¹ s⁻¹ (46), keeping the buffer concentrations low (≤2mM) assured that phosphate reactions with OH[•] would be negligible.

Analytical Techniques. Measurements of [OH[•]]_{ss} were accomplished using ¹⁴C-labeled formate as an OH[•] probe. In the presence of O₂, the formate anion reacts with OH[•] to produce CO₂ with a rate constant of 3.2 × 10⁹ M⁻¹ s⁻¹ (46). Formate does not react with O₂⁻, the only other radical present in significant steady-state concentrations during these radiolysis experiments (*k* < 0.01 M⁻¹ s⁻¹) (50). Irradiations were performed in glass scintillation vials with foil-

lined caps. To measure [^{14}C]formate remaining in solution, $^{14}\text{CO}_2$ was purged from the pH 6-buffered sample with argon prior to the addition of scintillation fluid in a 6:1 ratio of ScintiSafe Econo1 (Fisher Scientific) to sample. Scintillation counting was performed using a Beckman model 6500 scintillation counter.

Measurements of DIC were performed using a TOC-5000 (Shimadzu Corp.) in IC mode. To eliminate the interference of N_2O during the near-infrared (NDIR) detection of CO_2 , all samples were purged with argon following the addition of CO_2 -free NaOH to prevent the loss of the CO_2 . Measurements of DOC were performed using a TOC-5000 (Shimadzu Corp.) on samples acidified with concentrated HCl to $\text{pH} \leq 1$. Samples to be analyzed were purged for 4 min using CO_2 -free air (TOC grade) to remove DIC prior to injection. Optical spectra were obtained on a HP8453 diode-array spectrophotometer (Agilent Technology) using 10-cm quartz cuvettes and referenced to Milli-Q water. Hydrogen peroxide was analyzed using the chemiluminescent acridinium ester method (48).

Determination of LMW Carboxylic Acids. LMW carboxylic acids were determined by HPLC of their 2-nitrophenylhydrazide derivatives (51–53). The HPLC separation was optimized to detect a set of carboxylic acids previously observed to be produced by the irradiation of natural waters or aqueous solutions of humic materials: formic, acetic, oxalic, malonic, and levulinic acids (3, 12, 54, 55).

2-Nitrophenylhydrazine (2-NPH) was purchased from Acros Organics and was recrystallized from hot water, removed from the supernatant by filtration, and stored as a wet paste at room temperature until use. 1-Ethyl-3-(3-dimethylaminopropyl) carbodiimide hydrochloride (SigmaUltra grade) (EDC) was obtained from Sigma Chemical Company. Pyridine (99.9+%) and concentrated HCl (99.999%) were obtained from Aldrich Chemicals and used without further purification. Stock solution of the 2-NPH (0.050 M in 0.25 M HCl) and EDC (0.30 M) were made in advance and frozen in 5–10-mL aliquots, which were defrosted immediately prior to use. Concentrated HCl and pyridine were mixed in 1:1.25 volume ratio to make the derivatization reaction buffer. In our low alkalinity samples, this gave a reaction pH of 4.5, which is ideal for the derivatization reaction (52, 56).

The derivatization reaction was carried out in acid-washed (10% HNO_3 overnight), rinsed (UV treated 18 M Ω water), and combusted (450 °C for 12 h) 8-mL glass vials with Teflon-lined silicone septa closures (acid-washed and rinsed). The 0.1 mL of buffer, 0.1 mL of EDC stock, and 0.2 mL of 2-NPH stock were added (in order) per 1 mL of sample and allowed to stand in the dark at room temperature for 1.5 h. The 0.1 mL of 40% w/w KOH (SigmaUltra) per 1 mL of sample was then added, and the vial was heated at 70 °C for 10 min in a water bath. The derivatized sample was either analyzed immediately or stored overnight at 4 °C.

The various acids derivatives were quantified using a Hewlett-Packard 1150 HPLC system. The samples were preconcentrated on a polymeric reversed-phase guard column (Dionex IonPac NG1 10 μm , 4 \times 35 mm) used in place of the manual injector sample loop (52). A total of 100 μL of sample was passed through the concentrator column, followed by 1.0 mL of water to expel the alkaline derivatization reaction medium and remove some interfering reaction byproducts.

Separation used an isocratic ion-pairing eluent with a reversed-phase column (Phenomenex Luna 5 μm C18(2), 250 \times 4.6 mm) and guard cartridge (Phenomenex Securityguard C18, 4 \times 3.0 mm). The mobile phase consisted of 20% acetonitrile and 80% aqueous phase containing 7.5 mM tetrabutylammonium bromide and 3 mM phosphate at pH

7.0. This system gave baseline resolution of the five acids in 35 min.

The derivatives were detected by absorbance at 230 and 400 nm. Quantitation used external standardization with solutions containing known concentrations of the derivatives of the pure acids and SRFA or SRHA in the same concentration as in the related experiments. The system responded linearly up to 100 μM , with a detection limit of approximately 100 nM. It should be noted that even the high concentration of humic substances used here do not interfere in the determination of the small organic acids using this method. It is not surprising that the presence of measurable concentrations of LMW acids in unirradiated SRFA and SRHA solutions has not been previously reported, as the concentration of acids observed in these solutions is less than 0.2% of the total organic carbon.

Bioassays. Dilution cultures were prepared from Massachusetts Bay water sampled at Revere State Beach filtered through precombusted Whatman GF/F filters (3 h at 450 °C, nominal pore-size 0.7 μm) to remove bacterivorous protists. This filtering also resulted in a reduction in bacterial abundance from 6×10^6 to 6×10^5 cells mL^{-1} . The final concentration of DOC in the filtered sample was 3.6 mg of C L^{-1} (300 $\mu\text{M C}$). This coastal water was amended with filter-sterilized aqueous solutions of SRHA (36 mg of C L^{-1} , 3 mM C) and SRFA (45 mg of C L^{-1} , 3.75 mM C) dissolved in Milli-Q water. Identical solutions of SRHA (36 mg of C L^{-1}) and SRFA (45 mg of C L^{-1}) that had been exposed to γ -radiolysis for 30 min (approximately 30 $\mu\text{M OH}^\bullet$) as described above were also added to seawater (γ -SRHA, γ -SRFA). In each case, one part of humic or fulvic solution was added to 3 parts of seawater (v/v) so that the final DOC concentrations in the incubated cultures were 11.7 mg of C L^{-1} (SRHA) and 14.1 mg of C L^{-1} (SRFA), of which 2.7 mg of C L^{-1} (225 $\mu\text{M C}$) was from the DOC originally present in the coastal seawater. Each culture was also amended with NaH_2PO_4 and NH_4Cl to final N and P concentrations of 100 μM to achieve carbon limited growth conditions. For each amendment, triplicate cultures were incubated in darkness at 23 °C in acid-washed glass bottles sealed with Teflon-lined screw caps. Samples for bacterial abundance were taken daily from the cultures during the 6-day incubation and were preserved by adding 0.2 μm of filtered sodium tetraborate buffered formaldehyde to 2% final concentration. Samples were kept at 4 °C until analysis (within 2 weeks). As a result of the γ -radiolysis, initial hydrogen peroxide concentrations were 1.8 μM but declined to less than 500 nM by the fourth day of the incubation.

Bacterial abundance was analyzed using a FACScan flowcytometer (Becton Dickinson) (57). Samples containing formaldehyde-fixed bacterial cells were stained with the nucleic acid stain Syto 13 (50 μM final concentration, Molecular Probes). Counting was performed at low flow (12 $\mu\text{L min}^{-1}$) with detector voltages set to 400 (side scatter) and 560 (green fluorescence). Fluorescent microspheres (Carboxy YG, 1.58 μm diameter, Polysciences) were added to all samples at a final concentration of 4.5×10^6 beads mL^{-1} for use as internal reference. Cells were separated from fluorescent beads in a log–log dot plot of side scatter and green fluorescence, and bacterial cell abundance was determined using the fluorescent beads as an internal standard. Samples were run for 20 s or until a minimum of 2000 beads had been counted.

Epifluorescence microscopy and image analysis were used to estimate bacterial cell size and to ensure that predatory flagellates were absent in the cultures at the end of the incubations. Formaldehyde-fixed bacterial samples were stained with 4',6-diamidino-2-phenylindole (DAPI) (58), and cells were visualized with an Axioskop 2 fluorescence microscope (Zeiss) equipped with an Atto-Arc variable light source. For each culture, duplicate images were acquired

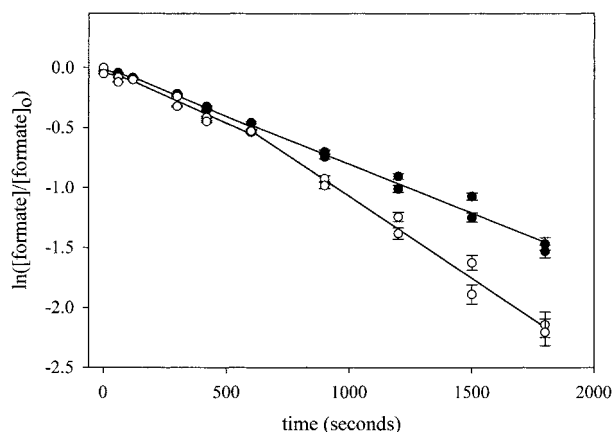


FIGURE 1. Mineralization of [^{14}C]formate in 5 mg of C L^{-1} SRFA (●) and SRHA (○) solutions saturated with N_2O and O_2 (4:1) and buffered to pH 6 with phosphate. Initial ^{14}C counts are 8000 and 7800 dpm for SRFA and SRHA, respectively, approximately 42 nCi (100 nM formate). The error bars are derived from counting statistics.

TABLE 1. OH^\bullet Reaction Rate Constants with SRFA and SRHA as a Function of Cumulative OH^\bullet Exposure^a

OH^\bullet range	SRFA (10^4 s^{-1} (mg of C L^{-1}))	SRHA (10^4 s^{-1} (mg of C L^{-1}))
early (0–2 μM)	3.8 (0.6)	3.8 (1.8)
middle (5.2–10.3 μM)	2.5 (0.1)	2.4 (0.2)
late (15.5–30.9 μM)	2.7 (0.2)	1.6 (0.07)
all data	2.7 (0.05)	1.9 (0.05)

^a Standard errors derived from the slopes of the lines in Figure 1 are in parentheses.

with a Magnafire cooled CCD camera (Optronics). Images were exported to the Scion Image 4.0.2 image analysis software, and an edge detection operator was used to define individual area, length, and width of > 100 cells per individual culture. Cell volumes were then estimated by approximating the shape of bacterial cells as a cylindrical cell with hemispherical end caps. Volumes were converted to bacterial carbon biomass for individual cells using the volume to dry weight relationship previously reported by Loferer-Kröb-bacher et al. (59) and assuming that carbon comprises 50% of the bacterial dry weight. Total bacterial carbon was calculated using bacterial abundance and average carbon content per cell in individual cultures.

Results

We have determined the second-order reaction rate coefficients for OH^\bullet with 5 mg of C/L (416 μM C) SRFA and SRHA using ^{14}C -labeled formate as a probe for OH^\bullet in solutions of the acids saturated with a 4:1 $\text{N}_2\text{O}/\text{O}_2$ mixture and buffered at pH 6. By utilizing [^{14}C]formate, we can add very small probe concentrations (100 nM), and as DOM is the only significant sink of OH^\bullet in this system, we can assume that the OH^\bullet steady-state concentration ($[\text{OH}^\bullet]_{\text{ss}}$) is determined by the scavenging rate of the DOM in the system. The concentration of formate anion after irradiation time t , $[\text{formate}]_t$, is described by

$$\ln [\text{formate}]_t / [\text{formate}]_0 = -k_{\text{formate}} [\text{OH}^\bullet]_{\text{ss}} t \quad (9)$$

where $[\text{formate}]_0$ is the initial formate concentration and k_{formate} is the second-order rate constant of reaction of OH^\bullet with formate (the reaction of OH^\bullet with formic acid is insignificant at this pH). If $[\text{OH}^\bullet]_{\text{ss}}$ is constant, a plot of $\ln[\text{formate}]_t / [\text{formate}]_0$ versus t should be linear, and $[\text{OH}^\bullet]_{\text{ss}}$ can then be obtained from the slope. Since the OH^\bullet

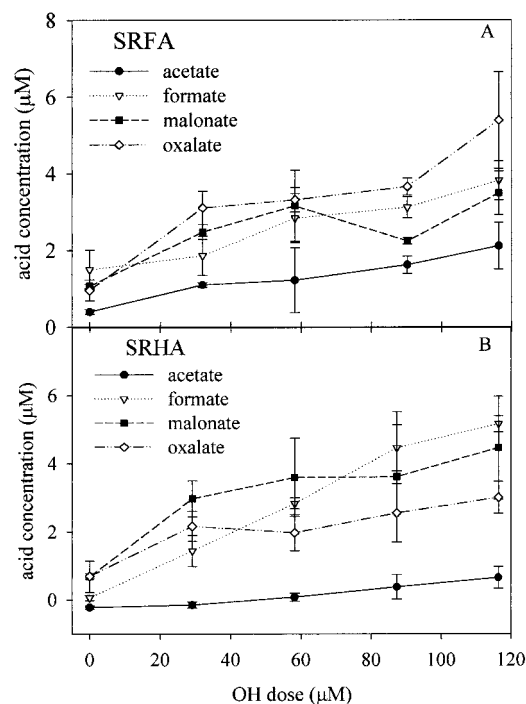


FIGURE 2. Measured formation of formic (▽), acetic (●), malonic (■), and oxalic (◇) acids from the reaction of OH^\bullet with SRFA (A) and SRHA (B). Error bars represent one standard deviation from the mean values of three separate irradiations. The analytical error for each determination would be smaller than the symbol.

TABLE 2. Ratio of Mole of Carboxylic Acid Produced per Mole of OH^\bullet for SRFA (14.0 mg of C L^{-1}) and SRHA (14.2 mg of C L^{-1})^a

acid	acid produced per OH^\bullet	
	SRFA	SRHA
formic	0.020 (0.003)	0.045 (0.003)
formic (corrected)	0.031	0.061
acetic	0.013 (0.003)	0.008 (0.001)
malonic	0.017 (0.005)	0.028 (0.008)
oxalic	0.032 (0.005)	0.017 (0.004)
total C	0.17	0.19

^a Ratios were calculated by linear regression of the individual experiments for which the average values are shown in Figure 2. Numbers in brackets are the standard errors of the slopes calculated during the regression analysis. Corrected formic acid production ratios from SRFA and SRHA were calculated by assuming that the maximum formate concentrations represent steady-state concentrations and using calculated $[\text{OH}^\bullet]_{\text{ss}}$ to obtain formate production rates (see Results). Losses of other acids via reaction with OH^\bullet are less significant as compared to formation rates and were neglected.

production rate P_{OH} in our radiolysis apparatus is known ($1.7 \times 10^{-8} \text{ M s}^{-1}$ in the presence of O_2), $[\text{OH}^\bullet]_{\text{ss}}$ can then be used to determine the sum of the rates of the reactions of OH^\bullet with its sinks, where each rate is given by the second-order rate constant of the reaction of OH^\bullet with sink i , $k_{\text{S},i}$, multiplied by the concentration of the sink, $[\text{S}]_i$:

$$\sum k_{\text{S},i} [\text{S}]_i = P_{\text{OH}} / [\text{OH}^\bullet]_{\text{ss}} \quad (10)$$

Plots of $\ln[\text{formate}]_t / [\text{formate}]_0$ versus irradiation time in fulvic and humic acid solutions exhibit a slope becoming steeper with increasing irradiation time, indicating that $[\text{OH}^\bullet]_{\text{ss}}$ is also increasing (Figure 1) and therefore that $\sum k_{\text{S},i} [\text{S}]_i$ is decreasing. Values of $\sum k_{\text{S},i} [\text{S}]_i$ calculated from the observed slopes all greatly exceeded the contributions of formate and phosphate species to the sum, showing that

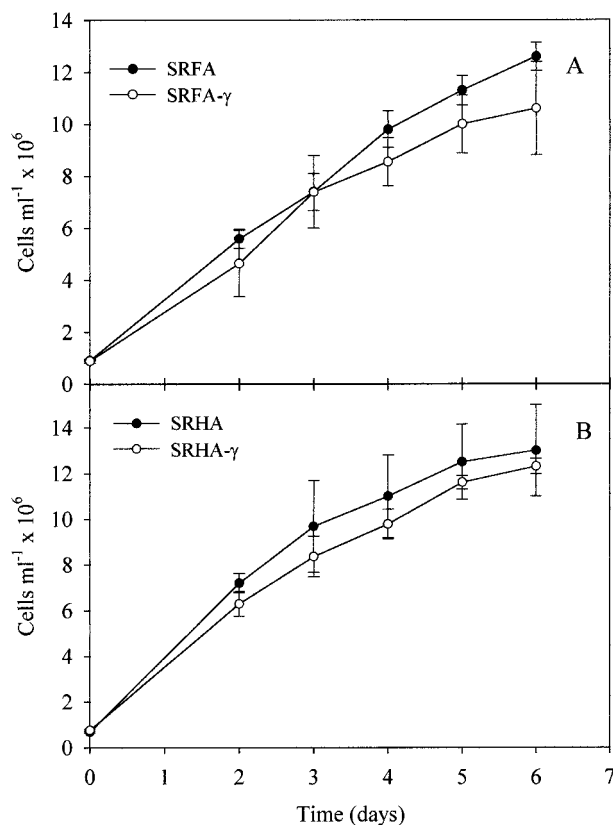


FIGURE 3. Average bacterial abundance in incubated cultures of GF/F filtered seawater amended 25% (v/v) with SRHA (A) or SRFA (B) with (○) or without (●) γ -radiolysis treatment. Initial DOC concentrations were 11.7 mg of C L⁻¹ for SRHA cultures and 14.1 mg of C L⁻¹ for SRFA cultures, of which 2.7 mg of C L⁻¹ was from the seawater inoculum and the rest from the humic substances. Error bars represent the standard deviation of triplicate incubations.

DOM is the only significant sink of OH[•] in this system and that $\sum k_{s,i}[S]_i$ is therefore equal to $k_{\text{DOM}}[\text{DOM}]$. DIC measurements (see below) indicate that [DOM] did not decrease significantly during the course of this experiment, so that the observed decreases in $\sum k_{s,i}[S]_i$ with longer irradiation time must be due to decreases in k_{DOM} . Calculated k_{DOM} values for SRFA and SRHA in the early, middle, and later parts of the irradiations (normalized to carbon content) are shown in Table 1.

We have observed the production of LMW carbon acids during the reaction of OH[•] with SRFA and SRHA (Figure 2). Production rates of acetic, formic, malonic, and oxalic acids per mole of OH[•] were approximately constant in the SRFA and in the SRHA solutions (Figure 2). Production rates of these acids determined from least squares regression of the data are shown in Table 2. No production of levulinic acid was observed in our experiments. The large flux of OH[•] used in these experiments could also react with the acids, reducing their observed concentration, and cause an underestimation of their production rates. However, maximum loss rates from reaction with OH[•] of oxalic and acetic acids were less than 4% of the net production rates shown in Table 2 ($[\text{OH}^{\bullet}]_{\text{ss}} = 4\text{--}6 \times 10^{-14}$ M, rate constants of deprotonated acids with OH[•] < 10^8 M⁻¹ s⁻¹; 50). The loss rate of malonic acid is at most 17% of the production rate in the SRFA experiment and 18% in the SRHA experiment (rate constant of the malonate reaction with OH[•] is 3×10^8 M⁻¹ s⁻¹). In the case of formic acid, the rate of reaction with OH[•] is much faster (rate constant of formate 3×10^9 M⁻¹ s⁻¹; 46). The observed net formate production rates of 3.2×10^{-10} M s⁻¹ (SRFA) and 7.3×10^{-10} M s⁻¹ (SRHA) can be corrected for the loss of formate by two

independent methods. The half-life of loss due to reaction with OH[•] is 60 min (SRHA) or 90 min (SRFA), so that approach of a formate steady-state concentration might be expected in our 120-min irradiation experiments. By assuming that the maximum formate concentration represents a steady-state concentration and using calculated $[\text{OH}^{\bullet}]_{\text{ss}}$ concentrations of 4×10^{-14} M (SRFA) and 6×10^{-14} M (SRHA), formate production rates of 4.9×10^{-10} M s⁻¹ (SRFA) and 9.9×10^{-10} M s⁻¹ (SRHA) can be calculated. Dividing these calculated formation rates by the OH[•] production rate of 1.6×10^{-8} M s⁻¹ leads to the calculated production ratio of 0.03 μM formic acid/ μM OH[•] for SRFA and the corresponding SRHA value of 0.06 μM acid/ μM OH[•] (Table 2). The larger correction for the SRHA solutions is due to the lower reaction rate constant of OH[•] with SRHA and hence a larger calculated $[\text{OH}^{\bullet}]_{\text{ss}}$. These revised rates can be arrived at independently by calculating the formate loss rate at each time point and performing a linear regression of the resulting corrected data. The values arrived at by this method are within 2% of those derived from the steady-state calculation.

The microbial growth experiment provided a measure of the total change in bioavailable substrates by the OH[•]-driven alteration of SRFA and SRHA. Samples exposed to 30 μM OH[•], a dose equivalent to 15 d of near-surface solar irradiation assuming a relatively high OH[•] production rate of 10^{-10} M s⁻¹ for 6 h/d (see Introduction), were inoculated with a natural consortium of coastal bacteria and incubated for 6 d. During the course of the 6-d incubation, bacterial abundance increased >10-fold in all cultures. There were no visible protozoan contaminants in any of the cultures at the end of this period. Radiolysis treatment of SRHA and SRFA resulted in a slightly lower bacterial abundance throughout the incubation (Figure 3), but neither the cell abundances nor the carbon content per cell differed significantly between irradiated samples and controls at maximum cell concentration (Students *t* test, $p > 0.1$; Table 3).

Radiolysis of the SRFA and SRHA solutions produced significant concentrations of DIC, showing that OH[•] and/or O₂⁻ reactions with DOM macromolecules are important in photomineralization processes. Since DIC production can be eliminated by the addition of *tert*-butyl alcohol, which scavenges OH[•] but not O₂⁻, OH[•] must be responsible for this mineralization (Figure 4). The rate of DIC production from a 0.5 mg of C L⁻¹ (42 μM DOC) solution of SRFA remains relatively constant until complete mineralization occurred (40 μM DIC produced, inset Figure 4). A further indication that neither O₂⁻ nor O₂ is responsible for a significant portion of the DIC production comes from the fact that there is only a small decrease in the DIC production rate when O₂ is excluded from the radiolysis experiments, as shown in Figure 5. The molar ratio of DIC produced to OH[•] generated is approximately 0.3 both in the SRFA solutions and in the SRHA solutions. This ratio is not significantly altered within the range of pH values found in natural waters (pH 4–10).

OH[•] radical reacts very rapidly with Br⁻ in seawater (60) and in other bromide-containing natural waters (61) to produce Br₂⁻ and BrO⁻, which may then react with CO₃²⁻ to produce the CO₃⁻ radical (60, 62). Any of these intermediate radicals may react more selectively with DOM than OH[•] does. Large concentrations of added Br⁻ (up to 0.1M) do not affect the production of DIC (Figure 5), indicating that these intermediate radicals are as effective as OH[•] in mineralizing DOM. Bromine species (BrO⁻ and BrOH) have been shown to be rapidly reduced by DOM at doses of 1.6 μM (mg of C L⁻¹)⁻¹ (63). Thus, although >97% of OH[•] in seawater reacts initially with Br⁻ (60), the final sink of these radicals is most likely DOM.

OH[•] was observed to be capable of bleaching SRFA and SRHA in the UV-B region of CDOM (300 nm) at a rate of approximately $2.1 (\pm 0.1) \times 10^4$ m⁻¹/M OH[•] produced for

TABLE 3. Initial DOC Measured in Dilution Culture Bioassays and Bacterial Abundance, Cellular Carbon Content, and Total Bacterial Carbon at Day 6 (Final Day of the Dilution Culture Bioassay)^a

material	treatment	initial DOC	bacterial biomass		
		(mg of C L ⁻¹)	(cells mL ⁻¹)	(fg of C cell ⁻¹)	(mg of C L ⁻¹)
SRHA	control	11.7	1.3 × 10 ⁷ (0.2 × 10 ⁷)	82 (34)	1.0 (0.4)
	γ	11.7	1.2 × 10 ⁷ (0.03 × 10 ⁷)	91 (8)	1.1 (0.1)
SRFA	control	14.1	1.3 × 10 ⁷ (0.05 × 10 ⁷)	102 (16)	1.2 (0.2)
	γ	14.0	1.1 × 10 ⁷ (0.2 × 10 ⁷)	106 (24)	1.1 (0.2)

^a Mean values of triplicate incubations are given with standard deviations in parentheses.

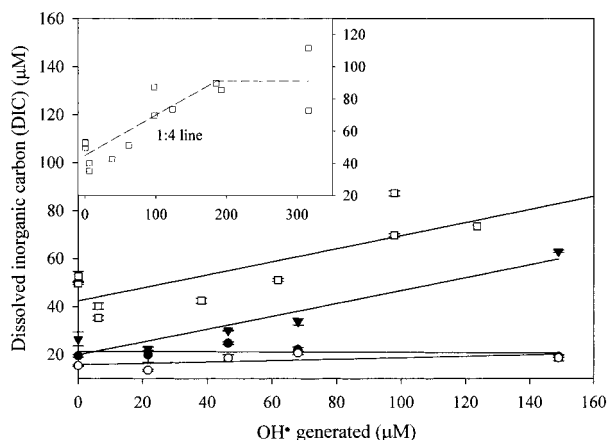


FIGURE 4. DIC production from irradiated SRFA (5 mg of C L⁻¹ (430 μM C), 2 mM phosphate buffer at pH 6), without (▼) and with (○) 0.3 M *tert*-butyl alcohol as a radical scavenger. Also shown is the lack of production of DIC from 0.3 M *tert*-butyl alcohol (●). Solid lines are linear fits to all the data. DIC is produced at a similar rate from a lower concentration of SRFA (□, 0.5 mg of C L⁻¹ (43 μM C)). The inset shows the complete mineralization of the 43 μM C SRFA solution at very high OH[•]. The dashed lines represent a theoretical formation rate of 1 mol of DIC/4 mol of OH[•] until complete mineralization of 43 μM C.

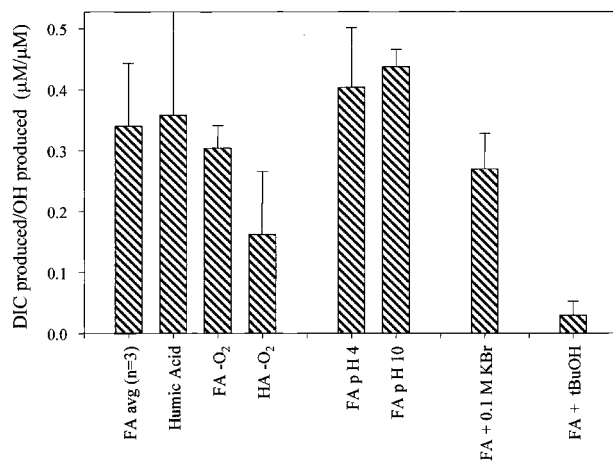


FIGURE 5. DIC production divided by OH[•] generated (μM/μM) for various treatments of SRFA and SRHA solutions. Unless specified otherwise, all solutions are 5 mg of C L⁻¹ (430 μM C) SRFA, 2 mM pH 6 phosphate buffer, and saturated with both N₂O and O₂. Error bars represent one standard deviation of the linear fits to the data.

SRFA and $4.3 (\pm 0.06) \times 10^4 \text{ m}^{-1}/\text{M OH}^\bullet$ for SRHA (Figure 6). Both DOC-free seawater amended with SRFA and coastal seawater samples from Delaware Bay exhibited similar bleaching rates ($1.3 (\pm 0.2) \times 10^4 \text{ m}^{-1}/\text{M OH}^\bullet$). These rates were only slightly lower than the bleaching observed in N₂O-saturated, buffered Milli-Q solutions of SRFA (Figure 6), although there is significant scatter, possibly due to pH

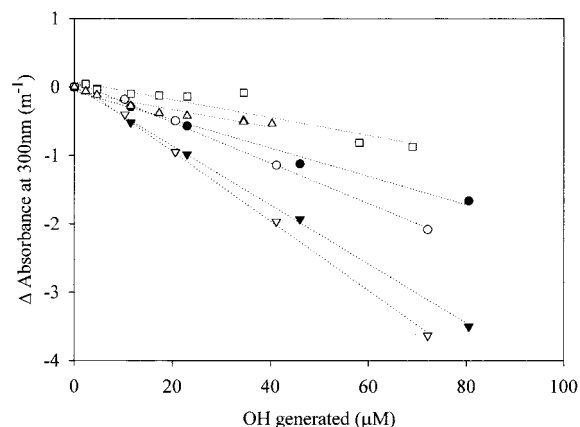


FIGURE 6. Bleaching of SRFA at 300 nm with (○) and without (●) oxygen, SRHA solutions with (▽) and without (▼) oxygen, DOC-free seawater amended with 5 mg of C L⁻¹ (430 μM C) SRFA prior to irradiation and saturated with N₂O/O₂ (□), and a coastal seawater sample from Delaware Bay saturated with N₂O/O₂ (△). All SRFA and SRHA solutions are 5 mg of C L⁻¹ (430 μM C), 2 mM pH 6 phosphate buffer, and saturated with N₂O or N₂O/O₂ as noted in the Methods. The dotted lines are linear fits (all $r^2 > 0.88$).

changes in these unbuffered solutions. The addition of O₂ to the radiolysis solutions increased the bleaching efficiency of OH[•] to $3.0 (\pm 0.1) \times 10^4 \text{ m}^{-1}/\text{M OH}^\bullet$ for SRFA and $5.1 (\pm 0.1) \times 10^4 \text{ m}^{-1}/\text{M OH}^\bullet$ for SRHA, possibly by increasing the efficiency of the OH[•]-mediated aromatic ring-opening reactions (see Discussion).

Discussion

The second-order reaction rate coefficients of OH[•] with SRFA and SRHA (k_{DOM}) determined in this work (Table 1) fall within the range of values for aquatic DOM determined by previous investigators ($(1-7) \times 10^4 \text{ s}^{-1}$) (20, 21, 64). Previous investigators have used similar techniques to determine the rate coefficients of the OH[•] reactions with SRFA and SRHA (23, 24). The rate constants determined were 30–40% lower than those found in this work but were determined at OH[•] doses that were 30% higher than used here. A decrease in the rate coefficients with increasing OH[•] dose, which cannot be accounted for by mineralization of the organic matter, has not been previously reported, although Peyton (65) speculated that this result might occur. The decrease is not unexpected, since these rate coefficients are the averages of the reaction rate constants of OH[•] with the many different constituent parts of the fulvic and humic acids. As the more rapidly reacting portions of the DOM are oxidized, the average rate coefficient decreases. The rate of DOM scavenging of OH[•] in natural waters, which often determines [OH[•]]_{ss}, should therefore be considered a function not only of the DOM concentration but also of the extent of DOM oxidation, although the magnitude of the effect that we observed is small compared to the variability in reactivity of DOM from different sources observed by others (20, 21, 23, 24, 28).

LMW Acid Production. OH[•] reactions with organic compounds fall into two basic mechanisms: addition (hydroxylation), generally to an aromatic ring, or hydrogen atom (H[•]) abstraction, both of which may lead to formation of LMW acids. Hydroxylation of aromatic moieties of the precursor material followed by ring opening can produce both mono- and diacids (35, 44, 66). Both hydroxylation and H[•] abstraction from phenols can break the aromaticity of an aromatic ring, forming hydroxycyclohexadienyl radicals (35, 44). Rearomatization is a significant driving force toward O₂/O₂⁻-driven scission of conjugated carbon-carbon bonds adjacent to the aromatic ring (C_α-C_β), leading to subsequent fragmentation and the formation of smaller oxidized products (see Figure 6 in ref 36). Another possible mechanism is H[•] abstraction from an unsaturated carbon-carbon bond to form a carbon-centered radical (R[•]) followed by reaction with O₂ to form a peroxy radical and subsequent decomposition to a carboxylic acid (67, 68).

We observed that the production of LMW acids from OH[•] reactions with SRFA was very similar to the rates observed in the SRHA solutions. In principle, SRFA represents a fraction of humic substances that contain more extensively substituted aromatic rings (69), which exhibit increased reactivity toward OH[•] (70), and are thus more easily broken down further by OH[•]. However, we did not observe large differences between SRFA and SRHA in the overall LMW acid production. Both SRFA and SRHA contain significant concentrations of carboxylic acid (11.2 vs 7.85 mol kg⁻¹) and phenolic (2.89 vs 1.86 mol kg⁻¹) residues (69). Substituted phenolic residues in particular might contribute to the production of LMW acids (35, 36).

Production of Bioavailable Carbon Substrates. The exposure of SRFA and SRHA samples to an environmentally relevant dose of OH[•] (30 μM) did not have any measurable effect on bacterial growth potential (differences between irradiated and unirradiated incubations 1 (± 2) × 10⁶ cells mL⁻¹, 0.1 (± 0.4) mg of C L⁻¹ for SRHA; 2 (± 2) × 10⁶ cells mL⁻¹, 0.1 (± 0.2) mg of C L⁻¹ for SRFA; Figure 3; Table 3). There is an extensive literature supporting a photochemically driven increase in bioavailability of terrestrially derived DOM such as humic materials (reviewed by Moran and Zepp; 71). Furthermore, OH[•] has been shown to selectively depolymerize cellulose in pulps (37) and has also been suggested to cleave cross-links in the rigid lignin matrix (34). Either of these mechanisms would serve to facilitate enzymatic degradation of high molecular weight DOM (e.g., humic and fulvic acids) into monomeric compounds that are available for bacterial utilization (45). In contrast, some recent studies have demonstrated that photochemical processes can have a negative impact on the ability of DOM to support bacterial growth (72-74), but these negative effects have generally been associated with the presence of more recent, algal-derived DOM and are therefore less likely to be significant in our experiment. While the simplest explanation of our result is that the reaction of DOM with OH[•] does not result in measurable formation of bioavailable products, we cannot rule out the possibility of counteractive positive and negative effects on DOM bioavailability with a zero net result.

The low production rates of LMW carbon acids by OH[•] are consistent with the lack of effect of OH[•] on bacterial growth in the bioassay results. The 30 μM dose of OH[•] used for the bioassay experiments would have produced total LMW acid carbon concentrations of ~0.07 mg of C L⁻¹ (5.5 μM C) in the solutions (Table 2). Conservatively assuming a 50% growth efficiency and a carbon content of 106 fg of C cell⁻¹ (Table 3), the carboxylic acid carbon produced in SRFA or in SRHA cultures could support the growth of 3.3 × 10⁵ cells. Although there is considerable uncertainty in the growth efficiency of microbial communities on carboxylic acids (range of 20-80%; 3), the formation rates of the LMW acids we measured

are clearly too low to be a significant source of bioavailable carbon in these experiments.

The bacterial growth in our dilution cultures suggests that a fraction of the added SRFA and SRHA was bioavailable; the yield of biomass we observed is consistent with what we would expect based on observations made on a variety of other humic materials (75, 76). While the contribution of the 2.7 mg of C L⁻¹ (300 μM C, 19-23% of total) DOC originally present from the Massachusetts Bay seawater is not clear, previous reports of "labile" fractions of natural aquatic DOM (19 ± 12% for marine DOM; 77) and an expected growth yield of less than 50% suggest that the bacterial growth is not attributable solely to this material.

DIC Production. Since the average oxidation state of carbon in SRFA and SRHA is approximately zero (69), an average DIC production rate of 0.25 mol of DIC/mol of OH[•] would be expected if OH[•] is the only oxidant participating in the mineralization reaction. Given the lack of effect of oxygen on the rate of mineralization, then the observed production of ~0.3 mol of DIC/mol of OH[•] is consistent with our expectations. The same is true in the presence of Br⁻, as long as Br⁻ is ultimately regenerated so that the overall outcomes of the reaction are reduction of OH[•] to OH⁻ and oxidation of DOM to DIC. Our parallel measurements of LMW acid production during irradiation show that production of DIC from OH[•] reaction with LMW acids is an insignificant fraction of the overall DIC formation rate, indicating that most of the mineralization of humic substances does not proceed via LMW acid intermediates. The observation that the rate of DIC production remains relatively constant from the beginning of the experiment until complete mineralization of the DOM (inset, Figure 4) suggests that breakdown of DOM into LMW molecules other than the LMW acids we measured is also not a necessary precursor for mineralization.

Bleaching. Bleaching (or fading) of CDOM is an important photoprocess that leads to increased light penetration into the water column and to decreased photochemical rates (since light must be absorbed in order to cause a photochemical reaction). The addition of O₂ to these solutions increases the bleaching rates of SRFA by 35% and SRHA by about 20% (Figure 6), possibly due to the formation of peroxy radicals followed by the decomposition of aromatic rings and conjugated double bonds. The presence of oxygen has been shown to increase the bleaching of paper pulps, most likely through a similar mechanism (35, 36, 38). Solutions of humic acids display increased bleaching relative to fulvic acid solutions (Figure 6). These differences may be due to the greater aromatic content of the humic reference material (78), which may be more readily bleached by OH[•] without being mineralized. Although the reactions of OH[•] with Br⁻ in seawater result in intermediates that we expected to react more selectively with chromophoric material, we did not observe an increase in the effectiveness of bleaching per OH[•] generated in seawater.

OH[•] As a Mechanism of DOM Photoproduct Formation. Assuming that the product formation efficiencies (mol of product/mol of OH[•]) for the materials we examined are similar to those for DOM from other sources, we can assess whether OH[•] could be a significant mechanism for photoformation of these products observed in previous studies. For example, in sunlight irradiation of water from Lake Skarshultsjon, a humic-rich, iron-rich Swedish lake (12.4 mg of C L⁻¹ (1.03 mM C), ~300 μg of Fe L⁻¹), a total LMW acid production rate of 1.6 μM C/h was observed, with formic acid being produced in greatest amount (3). In addition, photochemical irradiations of a series of lake waters showed that LMW acid carbon production was 20-30% of the concurrent DIC production (12). We observed formation of similar relative abundances of individual acids to each other and to DIC in both of these samples, including LMW acid carbon production rates of

30–40% of concurrent DIC production. Although it is difficult to generalize from SRFA and SRHA to other materials, if SRHA and Lake Skarshultsjon DOM behave similarly, a photoproduction rate of 8–9 $\mu\text{M OH}^*/\text{h}$ ($\sim 2 \times 10^{-9} \text{ M s}^{-1}$) would be required to produce the quantities of LMW acids and DIC observed to be photoproduced in Lake Skarshultsjon. Similarly, to explain the difference in DIC photoproduction in Satilla River water with and without addition of a ligand to eliminate Fe photoreactions (14), a difference in OH^* production rates of $\sim 16 \mu\text{M OH}^*/\text{h}$ is required if indirect, OH^* -mediated chemistry is solely responsible for the Fe-related DIC production. Based on these estimates, it seems unlikely that OH^* is responsible for a large fraction of the photochemical production of DIC or LMW acids observed in these waters. In addition, exposure to OH^* corresponding to an average solar exposure of 15 d (assuming OH^* photoproduction rates of $10^{-10} \text{ M s}^{-1}$ for 6 h/d) did not have any significant effect on bacterial growth potential (Figure 3; Table 3), in contrast to previous work that has shown enhanced bacterial growth potential after only 12 h of simulated surface UV radiation (74). Finally, for an OH^* production rate of $2 \mu\text{M d}^{-1}$ ($10^{-10} \text{ M s}^{-1}$ for 6 h/d), the maximum bleaching rate of SRFA and SRHA due to reactions with OH^* was $6 \times 10^{-2} \text{ m}^{-1} \text{ d}^{-1}$, less than 20% of photobleaching rates of $\sim 0.33 \text{ m}^{-1} \text{ d}^{-1}$ observed in similar solutions irradiated by simulated sunlight (79). Thus, indirect photobleaching of SRFA via the photointermediate OH^* is only a candidate as a significant mechanism of total photobleaching in waters with very high OH^* photoproduction rates, for example, in iron-rich acidic systems where Fenton chemistry may be important. To the extent that SRFA and SRHA are representative of aquatic DOM, we can eliminate OH^* reactions with humic substances as a significant mechanism for formation of DOM photoproducts.

Acknowledgments

We thank Phil Gschwend for the loan of the HPLC and Urs von Gunten and Michael Elovitz for helpful discussions. This work was funded by NSF-OCE 9819089. M.J.P. was supported by a NSF Earth Sciences Postdoctoral Fellowship. S.B. was supported by a Wallenberg Postdoctoral Fellowship. This is WHOI Publication No. 10468.

Literature Cited

- Zuo, Y.; Jones, R. D. *Naturwissenschaften* **1995**, *82*, 472–474.
- Zhou, X.; Mopper, K. *Mar. Chem.* **1997**, *56*, 201–213.
- Bertilsson, S.; Tranvik, L. *Limnol. Oceanogr.* **1998**, *43*, 885–895.
- Kieber, D. J.; Mopper, K. *Mar. Chem.* **1987**, *21*, 135–149.
- Kieber, R. J.; Zhou, X.; Mopper, K. *Limnol. Oceanogr.* **1990**, *35*, 1503–1515.
- Mopper, K.; Stahovec, W. L. *Mar. Chem.* **1986**, *19*, 305–321.
- Kieber, D. J.; McDaniel, J.; Mopper, K. *Nature* **1989**, *341*, 637–639.
- Bushaw, K. L.; Zepp, R. G.; Tarr, M. A.; Schulz-Janders, D.; Bourbonniere, R. A.; Hodson, R. E.; Miller, W. L.; Bronk, D. A.; Moran, M. A. *Nature* **1996**, *381*, 404–407.
- Williamson, C. E. *Limnol. Oceanogr.* **1995**, *40*, 386–392.
- Miller, W. L.; Zepp, R. G. *J. Geophys. Res.* **1995**, *22*, 417–420.
- Bertilsson, S.; Allard, B. *Arch. Hydrobiol./Adv. Limnol.* **1996**, *48*, 133–141.
- Bertilsson, S.; Tranvik, L. *Limnol. Oceanogr.* **2000**, *45*, 753–762.
- Bano, N.; Moran, M. A.; Hodson, R. E. *Aquat. Microb. Ecol.* **1998**, *16*, 95–102.
- Gao, H.; Zepp, R. G. *Environ. Sci. Technol.* **1998**, *32*, 2940–2946.
- Granéli, W.; Lindell, M.; Tranvik, L. *Limnol. Oceanogr.* **1996**, *41*, 698–706.
- Zafriou, O. C. *Chemical Oceanography*; Academic Press: London, 1983; Vol. 8.
- Zafriou, O. C.; Jousset-Dubien, J.; Zepp, R. G.; Zika, R. *Environ. Sci. Technol.* **1984**, *18*, 358A–371A.
- Blough, N. V.; Zepp, R. G. *Active Oxygen in Chemistry*; Foote, C. S., Valentine, J. S., Eds.; Chapman and Hall: New York, 1995; pp 280–333.
- Cooper, W. J.; Zika, R. G.; Petasne, R. G.; Fischer, A. M. *Aquatic Humic Substances: Influence on Fate and Treatment of Pollutants*; Suffet, I. H., MacCarthy, P., Eds.; American Chemical Society: Washington, DC, 1989; Advances in Chemistry Series 219.
- Brezonik, P. L.; Fulkerson-Brekken, J. *Environ. Sci. Technol.* **1998**, *32*, 3004–3010.
- Westerhoff, P.; Aiken, G.; Amy, G.; Debroux, J. *Water Res.* **1999**, *33*, 2265–2276.
- Zepp, R. G.; Hoigne, J.; Bader, H. *Environ. Sci. Technol.* **1987**, *21*, 443–450.
- Elovitz, M. S. personal communication.
- Elovitz, M. S.; von Gunten, U. *ACS Conference Proceedings—Division of Environmental Chemistry Preprints and Extended Abstracts*; American Chemical Society: Washington, DC, March 1999; Vol. 39, p 123.
- Wagner, I.; Strehlow, H.; Busse, G. *Z. Phys. Chem. (Munich)* **1980**, *123*, 1–33.
- Vaughn, P. P.; Blough, N. V. *Environ. Sci. Technol.* **1998**, *32*, 2947–2953.
- Mopper, K.; Zhou, X. *Science* **1990**, *250*, 661–664.
- Zepp, R. G.; Faust, B. C.; Hoigne, J. *Environ. Sci. Technol.* **1992**, *26*, 6.
- Voelker, B. M.; Morel, F. M. M.; Sulzberger, B. *Environ. Sci. Technol.* **1997**, *31*, 1004–1011.
- Southworth, B.; Voelker, B. M. unpublished data.
- Miles, C. J.; Brezonik, P. L. *Environ. Sci. Technol.* **1981**, *15*, 1089–1095.
- Faust, B. C.; Hoigne, J. *Atmos. Environ.* **1990**, *24A*, 79–89.
- Hobbs, G. C.; Abbot, J. J. *Wood Chem. Technol.* **1994**, *14*, 195–225.
- Gierer, J.; Jansbo, K. J. *Wood Chem. Technol.* **1993**, *13*, 561–581.
- Gierer, J. *Holzforchung* **1997**, *51*, 34–46.
- Gierer, J. *Lignin: Historical, Biological, and Materials Perspectives*; Glasser, W. G., Northey, R. A., Schultz, T. P., Eds.; ACS Symposium Series 742; American Chemical Society: Washington, DC, 2000.
- Chirat, C.; Lachemal, D. *Holzforchung* **1997**, *51*, 147–154.
- Ragnar, M.; Eriksson, T.; Reitberger, T. *Holzforchung* **1999**, *53*, 292–298.
- Staelin, J.; Hoigne, J. *Environ. Sci. Technol.* **1985**, *19*, 1206–1213.
- Hoigne, J.; Bader, H. *Water Res.* **1976**, *10*, 337–386.
- Hoigne, J. *The Handbook of Environmental Chemistry V5. Part C: Quality and Treatment of Drinking Water II*; Hrubec, J., Ed.; Springer-Verlag: Heidelberg, 1998.
- Gagnon, G. A.; Booth, S. D. J.; Peldszus, S.; Mutti, D.; Smith, F.; Huck, P. M. *J. Am. Water Works Assoc.* **1997**, *89*, 88–97.
- Kuo, C.-Y.; Wang, H.-C.; Krasner, S. W.; Davis, M. K. *Water Disinfection and Natural Organic Matter*; Minear, R. A., Amy, G. L., Eds.; ACS Symposium Series 649; American Chemical Society: Washington, DC, 1996.
- Lanzalunga, O.; Bietti, M. *J. Photochem. Photobiol. B: Biol.* **2000**, *56*, 85–108.
- Tranvik, L. J. *Aquatic Humic Substances: Ecology and Biogeochemistry*; Hessen, D. O., Tranvik, L. J., Eds.; Springer-Verlag: Berlin, 1998; pp 259–283.
- Buxton, G. V.; Greenstock, C. L.; Helman, W. P.; Ross, A. B. *J. Phys. Chem. Ref. Data* **1988**, *17*, 513–889.
- Spinks, J. W. T.; Woods, R. J. *An Introduction to Radiation Chemistry*, 3rd ed.; John Wiley & Sons: New York, 1990.
- Cooper, W. J.; Moegling, J. K.; Kieber, R. J.; Kiddle, J. J. *Mar. Chem.* **2000**, *70*, 191–200.
- Bader, H.; Sturzenegger, V.; Hoigne, J. *Water Res.* **1988**, *22*, 1109–1115.
- NDRL-RCDC. Notre Dame Radiation Laboratory Radiation Chemistry Data Center.
- Miwa, H.; Hiyama, C.; Yamamoto, M. *J. Chromatogr.* **1985**, *321*, 165–174.
- Albert, D. B.; Martens, C. S. *Mar. Chem.* **1997**, *56*, 27–37.
- Muellerharvey, I.; Parkes, R. J. *Estuarine Coastal Shelf Sci.* **1987**, *25*, 567–579.
- Wetzel, R. G.; Hatcher, P. G.; Bianchi, T. S. *Limnol. Oceanogr.* **1995**, *40*, 1369–1380.
- Bertilsson, S.; Bergh, S. *Chemosphere* **1999**, *39*, 2289–2300.
- Vairavamurthy, A.; Mopper, K. *Anal. Chim. Acta* **1990**, *237*, 215–221.
- del Giorgio, P. A.; Bird, D. F.; Prairie, Y. T.; Planas, D. *Limnol. Oceanogr.* **1996**, *41*, 783–789.
- Porter, K. G.; Feig, Y. S. *Limnol. Oceanogr.* **1980**, *25*, 943–948.
- Loferer-Kröbbacher, M.; Klima, J.; Psenner, R. *Appl. Environ. Microbiol.* **1998**, *64*.

- (60) Zafiriou, O. C.; True, M. B.; Hayon, E. *Photochemistry of Environmental Aquatic Systems*; Zika, R. G., Cooper, W. J., Eds.; American Chemical Society: Washington, DC, 1987.
- (61) von Gunten, U.; Hoigne, J. *Environ. Sci. Technol.* **1994**, *28*, 1234–1242.
- (62) True, M. B.; Zafiriou, O. C. *Photochemistry of Environmental Aquatic Systems*; Zika, R. G., Cooper, W. J., Eds.; ACS Symposium Series 327; American Chemical Society: Washington, DC, 1987; pp 106–115.
- (63) Song, R. G.; Westerhoff, P.; Minear, R. A.; Amy, G. L. *Water Disinfection and Natural Organic Matter*; ACS Symposium Series 649; American Chemical Society: Washington, DC, 1996; pp 298–321.
- (64) Hoigné, J.; Bader, H. *Ozone Sci. Eng.* **1979**, *1*.
- (65) Peyton, G. R. *Mar. Chem.* **1993**, *41*, 91–103.
- (66) Gopalan, S.; Savage, P. E. *J. Phys. Chem.* **1994**, *98*, 12646–12652.
- (67) von Sonntag, C.; Schuchmann, H.-P. *Peroxy Radicals*; Alfassi, Z. B., Ed.; John Wiley and Sons: New York, 1997.
- (68) Passi, S.; Picardo, M.; De Luca, C.; Nazzaro-Porro, M.; Rossi, L.; Rotilio, G. *Biochim. Biophys. Acta* **1993**, *1168*, 190–198.
- (69) I.H.S.S. Standard and Reference Collection, International Humic Substances Society, 2001.
- (70) Barnes, A. R.; Sugden, J. K. *Pharm. Acta Helv.* **1986**, *61*, 218–227.
- (71) Moran, M. A.; Zepp, R. G. *Limnol. Oceanogr.* **1997**, *42*, 1307–1316.
- (72) Benner, R.; Biddanda, B. *Limnol. Oceanogr.* **1998**, *43*, 1373–1378.
- (73) Obernosterer, I.; Reiner, B.; Herndl, G. J. *Limnol. Oceanogr.* **1999**, *44*, 1645–1654.
- (74) Tranvik, L. J.; Bertilsson, S. *Ecology Lett.* **2001**, *4*, 458–463.
- (75) Moran, M. A.; Hodson, R. E. *Limnol. Oceanogr.* **1990**, *35*, 1744–1756.
- (76) Sun, L.; Perdue, E. M.; Meyer, J. L.; Weis, J. *Limnol. Oceanogr.* **1997**, *42*, 714–721.
- (77) Søndergaard, M.; Middelboe, M. *Mar. Ecol. Prog. Ser.* **1995**, *118*, 283–294.
- (78) Ravichandran, M.; Aiken, G. R.; Reddy, M. M.; Ryan, J. N. *Environ. Sci. Technol.* **1998**, *32*, 3305–3311.
- (79) Goldstone, J. V.; Voelker, B. M. unpublished data.

Received for review May 9, 2001. Revised manuscript received October 9, 2001. Accepted October 16, 2001.

ES0109646